IHEP 2003-20

August 25, 2003

OEF

Search for light pseudoscalar sgoldstino in K^- decays

I.V. Ajinenko, S.A. Akimenko, I.G. Britvich, G.I. Britvich, K.V. Datsko, A.P. Filin, A.V. Inyakin, A.S. Konstantinov, V.F. Konstantinov, I.Y. Korolkov, V.M. Leontiev, V.P. Novikov, V.F. Obraztsov, V.A. Polyakov, V.I. Romanovsky, V.I. Shelikhov, N.E. Smirnov, O.G. Tchikilev, V.A. Uvarov, O.P. Yushchenko.

Institute for High Energy Physics, Protvino, Russia

V.N. Bolotov, S.V. Laptev, A.R. Pastsjak, A.Yu. Polyarush, R.Kh. Sirodeev.

Institute for Nuclear Research Moscow, Russia

Abstract

A search for the light pseudoscalar sgoldstino production in three-body K^- decay $K^- \to \pi^- \pi^0 \, P$ has been performed with the “ISTRA+” detector exposed to the 25 GeV negative secondary beam of the U-70 proton synchrotron. No signal is seen. Upper limit for the branching ratio $Br(K^- \to \pi^- \pi^0 P)$ at 90% confidence level is found to be $\sim 8 \cdot 10^{-6}$ in the effective mass m_P range $0 \div 200$ MeV, excluding the region near m_{π° where it degrades to $\sim 3 \cdot 10^{-5}$.

1 Introduction

In supersymmetric models with spontaneous supersymmetry breaking superpartners of a Goldstone fermion — goldstino, pseudoscalar P and scalar S, should exist. In various versions of gravity mediated and gauge mediated theories one or both of these weakly interacting bosons (sgoldstinos) are light and therefore can be observed in kaon decays. Moreover, if sgoldstino interactions with quarks conserve parity, (as in left-right extensions of MSSM), and P is lighter than S, so that $m_S > (m_K - m_\pi)$ and $m_P < (m_K - 2m_\pi)$, sgoldstinos show up in the decay $K \to \pi\pi P$(see Fig.1), rather than in a much better constrained $K \to \pi S$. The phenomenology of light sgoldstinos in this scenario is considered in detail in [1]. Under assumption that sgoldstino interactions with quarks and gluons violate quark flavor and conserve parity, low energy interactions of pseudoscalar sgoldstino P with quarks are described by the Lagrangian:

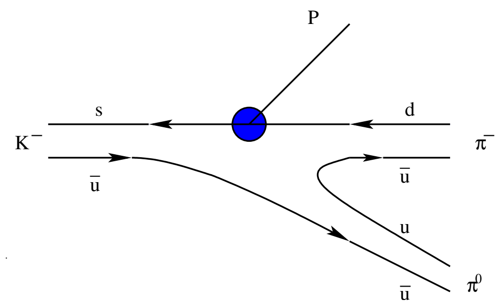

Figure 1: K^- decay into sgoldstino and pions.

$$L = -P \cdot (h_{ij}^D \cdot \overline{d}_i i\gamma^5 d_j + h_{ij}^U \cdot \overline{u}_i i\gamma^5 u_j) \tag{1}$$

with

$$d_i = (d, s, b) \,, \qquad u_i = (u, c, t) \,,$$

with coupling constants h_{ij} proportional to the left-right soft terms in the matrix of squared masses of squarks:

$$h_{ij}^D = \frac{\tilde{m}_{D,ij}^{(LR)2}}{\sqrt{2}F} \,, \qquad h_{ij}^U = \frac{\tilde{m}_{U,ij}^{(LR)2}}{\sqrt{2}F} \,, \tag{2}$$

here the scale of supersymmetry breaking is denoted as $\sqrt{F}$. The constraints on the flavor-violating coupling of sgoldstino to quarks is evaluated using the $K_L^\circ - K_S^\circ$ mass difference and CP violating parameter ϵ in the neutral kaon system: $|h_{12}^D| \leq 7 \cdot 10^{-8}$; $|Reh_{12}^D \cdot Imh_{12}^D| < 1.5 \cdot 10^{-17}$. It has been shown in [1] that, depending on the phase of sgoldstino-quark coupling, these constraints result in the following limits on the branching ratio: $Br(K^- \to \pi^-\pi^0 P) \leq 1.5 \times 10^{-6} \div 4 \times 10^{-4}$. A search for P in charged kaon decays is of particular interest for the case $Reh_{12}^D \sim 0$, when the corresponding branching ratio of K_L is small.

Light sgoldstino decays into two photons or into a pair of charged leptons, two photon decay dominating almost everywhere in the parameter space. Depending on the parameter $g_\gamma = \frac{1}{2\sqrt{2}}\frac{M_{\gamma\gamma}}{F}$, where $M_{\gamma\gamma}$ is the photino mass, sgoldstino decays either inside or outside the detector. In the present search we assume that sgoldstino decays outside the detector, i.e. is invisible. The existing limits on the branching $Br(K^- \to \pi^-\pi^0 P)$ are at the level of $4 \cdot 10^{-5}$ [2], whereas the limits for the scalar sgoldstino S can be estimated from the studies of the $K^+ \to \pi^+\nu\overline{\nu}$ at the level of $4.7 \cdot 10^{-9}$, see [3] for a recent review.

The aim of our present study is to search for invisible pseudoscalar sgoldstino in the decay of K^-. Experimental setup and event selection are described in Section 2, the results of the analysis are

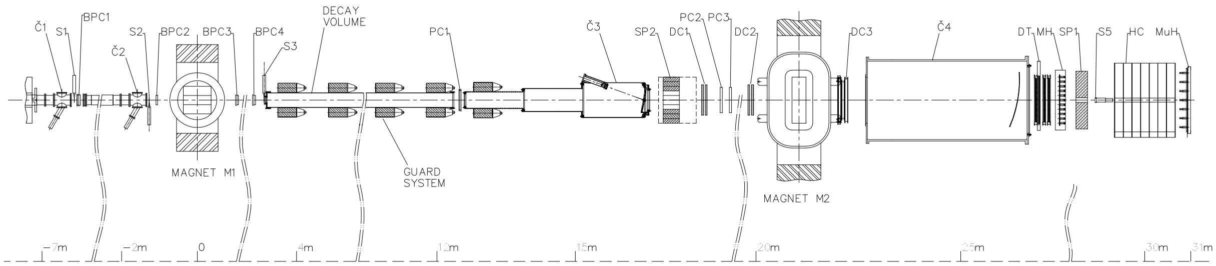

Figure 2: The elevation view of the ISTRA+ setup.

presented in Section 3 and the conclusions are given in the last Section. Preliminary results of this study have been presented in [4].

2 Experimental setup and event selection

The experiment is performed at the IHEP 70 GeV proton synchrotron U-70. The ISTRA+ spectrometer has been described in some detail in our recent papers on K_{e3} [5], $K_{\mu 3}$ [6] and $\pi^-\pi^\circ\pi^\circ$ decays [7], here we briefly recall characteristics relevant to our analysis. The ISTRA+ setup is located in the negative unseparated secondary beam line 4A of U-70. The beam momentum is ~ 25 GeV with $\Delta p/p \sim 1.5\%$. The admixture of K^- in the beam is $\sim 3\%$, the beam intensity is $\sim 3 \cdot 10^6$ per 1.9 sec U-70 spill. A schematic view of the ISTRA+ setup is shown in Fig. 2. The beam particles deflected by the magnet M_1 are measured by four proportional chambers BPC_1—BPC_4 with 1 mm wire step, the kaon identification is done by three threshold Cerenkov counters $\check{C}_0$—$\check{C}_2$. The 9 meter long vacuumed decay volume is surrounded by eight lead glass rings used to veto low energy photons. The same role is played by 72-cell lead glass calorimeter SP_2. The decay products deflected in the magnet M_2 with 1 Tm field integral are measured with 2 mm step proportional chambers PC_1—PC_3, with 1 cm cell drift chambers DC_1—DC_3 and finally with 2 cm diameter drift tubes DT_1—DT_4. A wide aperture threshold Cerenkov counters $\check{C}_3$,$\check{C}_4$,filled with He, serve to trigger electrons and are not used in the present measurement. SP_1 is a 576-cell lead glass calorimeter, followed by HC — a scintillator-iron sampling hadron calorimeter. MH is a 11x11 cell scintillating hodoscope, used to improve the time resolution of the tracking system, MuH is a 7x7 cell muon hodoscope.

The trigger is provided by scintillation counters S_1—S_5, beam Cerenkov counters and by the analog sum of amplitudes from last dinodes of the SP_1 : T=$S_1 \cdot S_2 \cdot S_3 \cdot \overline{S}_4 \cdot \check{C}_1 \cdot \overline{\check{C}}_2 \cdot \overline{\check{C}}_3 \cdot \overline{S}_5 \cdot \Sigma(SP_1)$, here S_4 is a scintillation counter with a hole to suppress beam halo, S_5 is a counter downstream of the setup at the beam focus, $\Sigma(SP_1)$ - a requirement for the analog sum to be larger than a MIP signal.

During first run in March-April 2001, 363 million of trigger events were logged on DLT's. During second physics run in November-December 2001 350 million trigger events were collected with higher beam intensity and stronger trigger requirements. This information is supported by about 300M MC events generated using Geant3 [8] for dominant K^- decay modes. Signal efficiency for possible sgoldstino production has been estimated using one million generated events for the first run configuration and 0.5 million events for the second run configuration, for each effective mass m_P point in the mass interval from 0 to 200 MeV with a step of 10 MeV. These signal events were weighted using the matrix element given in [1].

Data collected in two runs, Spring 2001, first run, and Winter 2001, second run, are used. Some information on the data processing and reconstruction procedures is given in [5, 6, 7], here we briefly mention the details, relevant for $\pi^-\pi^\circ$ + missing energy event selection. Part of technical distributions, omitted in the present paper, has been shown in [4].

The muon identification (see [6]) is based on the information from the SP_1 — a 576-cell lead glass calorimeter and the HC — a scintillation-iron sampling calorimeter. The electron identification (see [5]) is done using E/p ratio — of the energy of the shower associated with charged track and charged track momentum.

A set of cuts is designed in order to suppress various backgrounds to possible sgoldstino production:

0) Events with one reconstructed charged track and with two electromagnetic showers in the electromagnetic calorimeter SP_1 are selected. We require the effective mass m$(\gamma\gamma)$ to be within ± 50 MeV from m_{π°. Events with vertex inside interval $400 < z < 1650$ cm are selected.

1) "Soft" charged pion identification is applied, tracks having electron or muon flag (as described in [5, 6]) are rejected.

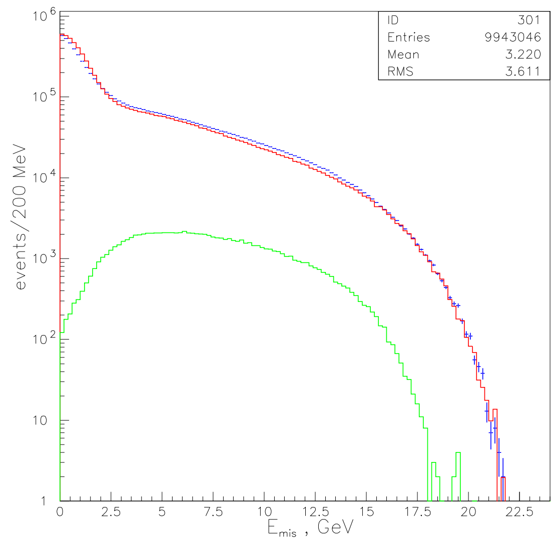

Figure 3: Missing energy spectra, second run data. Points show real data, upper histogram — background MC events, lower histogram — signal MC events for $m_P = 90$ MeV.

2) Events with missing energy $E_{beam} - E_{\pi^-} - E_{\pi^\circ}$ above 3 GeV are selected. This cut serves to reduce the $K_{\pi 2}$ contamination. In Fig. 3 missing energy spectra for the second run data, MC background and MC signal with m_P of 90 MeV are compared.

3) To reduce the charged particles background in the photon sample, the MH information is used. The distance r between SP1 shower and the nearest MH hit in the plane transverse to the beam is shown in Fig. 4. The events are selected where at least one shower has this distance above 10 cm.

4) The events where one of the photons is suspected to be irradiated by the charged particle in a detector material upstream/inside M2-magnet are rejected.

Such photons have nearly the same x coordinate(in the direction of the magnetic field) as the charged track on the SP_1 face, i.e. an event is rejected if for one or both showers $\Delta x = |x_{ch} - x_\gamma| < 7$ cm and $\Delta y = |y_{ch} - y_\gamma| < 30$ cm.

5) Events having good K_{e3} 2C-fit are removed.

6) To suppress the tails from the $K_{\pi 2}$ decay a cut on the charged pion momentum p^* in the kaon rest frame $p^*(\pi^-) < 180$ MeV is applied.

7) The pion identification , mainly based on the HC information is required . The efficiency and muon suppression of this selection has been determined using $K_{\mu 2}$ and $K_{\pi 2}$ decays. The efficiency is found to be 70 % and 80 % for the first and second run data respectively. The remaining muon admixture is equal to 3 % and 2 %.

8) To suppress $\pi^-\pi^\circ\gamma$ background only the events with missing momentum pointing to SP_1 transverse plane within SP_1 working aperture are selected.

9) The "Veto" cut uses information from the Guard System GS and the guard electromagnetic calorimeter SP_2: absence of signals above noise threshold is required.

The data reduction information for the second run is given in Table 1 and is compared there with MC-background statistics and with MC-signal statistics for the sgoldstino mass of $m_P = 90$ MeV. The cut suppression factors w_{i-1}/w_i for the MC data are calculated using the corresponding matrix elements.

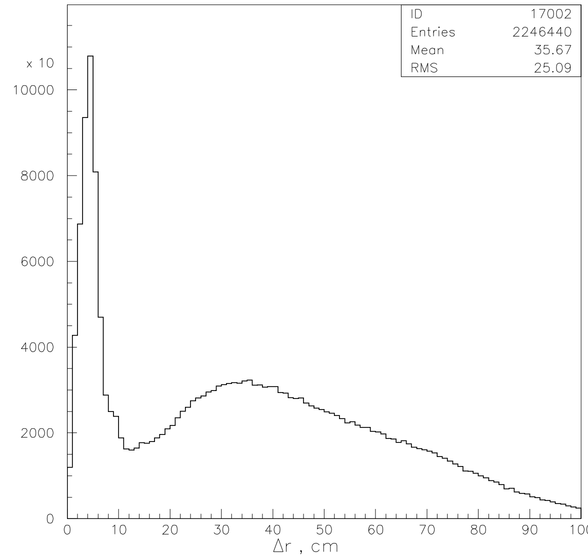

Figure 4: The distance r between the SP1 shower and the nearest MH hit, second run data.

The influence of the last cuts on the missing mass squared spectra $(P_K - P_{\pi^-} - P_{\pi^\circ})^2$, which is used as the signal "estimator", is shown in Fig. 5. The left wide bump in Fig. 5 is due to $K_{\mu 3}$ decays, the shift to negative missing mass squared is caused by the use of the pion mass in its calculations. Second peak is caused by $\pi^-\pi^\circ(\pi^\circ)$ decay with gammas from second π° escaping detection. No evidence for additional sgoldstino signal is seen.

Table 1: Event reduction statistics for the second run.

Cut	real data	N_{i-1}/N_i	BG MC	w_{i-1}/w_i	MC m_P=90 MeV	w_{i-1}/w_i
(0) 1 π^-, m$(\gamma\gamma)$ near m(π°)	9943046		5512890		98289	
(1) no (e, μ)	7771606	1.28	4545059	1.19	93470	1.05
(2) $E_{mis} > 3.0$ GeV	1123220	6.92	588735	7.78	82602	1.17
(3) MH filter	939052	1.20	516922	1.19	74744	1.09
(4) conv. gammas	722622	1.30	426286	1.22	56513	1.25
(5) no K_{e3} fit	458338	1.58	201580	2.27	35906	1.69
(6) $p^*(\pi^-) < 180$ MeV	326935	1.40	134706	1.28	35698	1.01
(7)π^- identification	122804	2.66	68380	2.06	33401	1.06
(8) $10 < rr < 60$ cm	108992	1.13	60698	1.12	31431	1.06
(9) Veto	31451	3.47	18674	3.58	31104	1.01

As a result of the previous cuts, especially the last "Veto" cut, π°-signal practically disappears

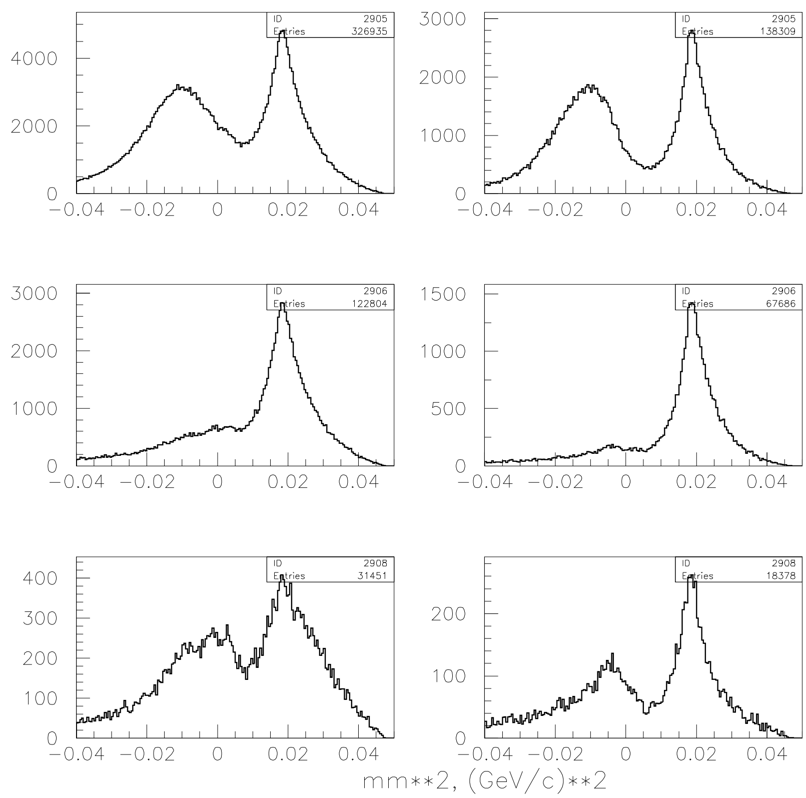

Figure 5: Missing mass squared distributions after cuts 6, 7 and 9, left column — second run data, right column — MC for dominant K^- decay modes. The bin size is equal to 0.0005 (GeV/c)^2.

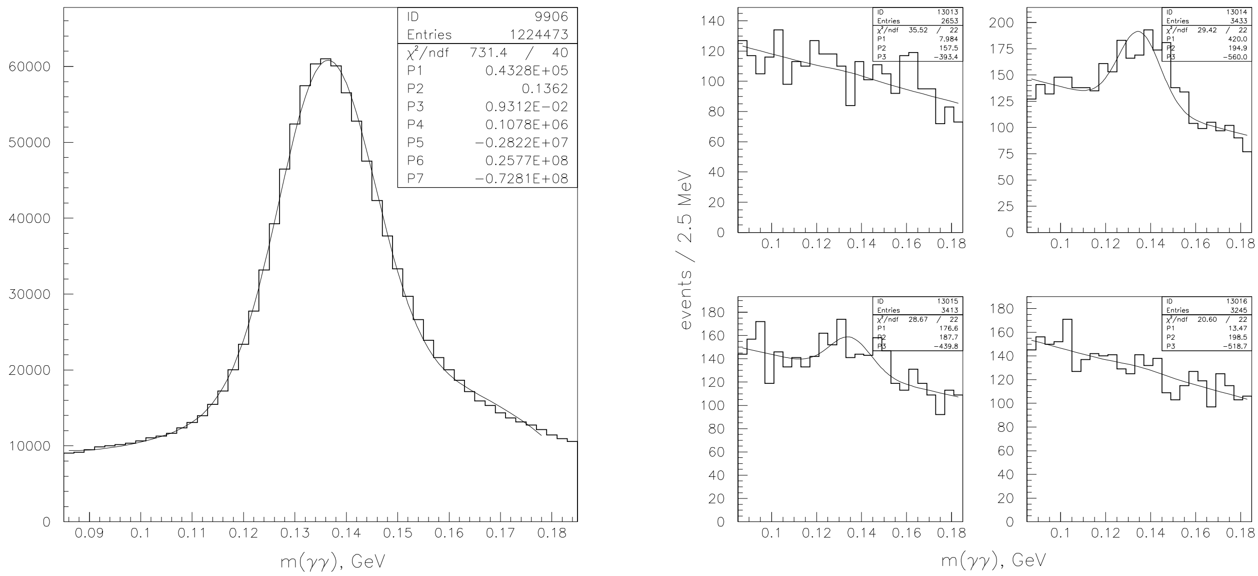

Figure 6: $m(\gamma\gamma)$ spectrum for events with $E_{mis} > 3.0$ GeV with the results of the fit by the sum of the Gaussian and third degree polynomial(left part); $m(\gamma\gamma)$ spectra after the "Veto" cut for the missing mass m_P intervals 120-130, 130-140, 140-150 and 150-160 MeV(right part), run 1 plus run 2 data.

from the $\gamma\gamma$ mass spectrum for certain missing mass (m_P) intervals. To illustrate that, the $m(\gamma\gamma)$ spectrum after cut (2) is shown in Fig. 6(left half). The right half of Fig. 6 shows the $\gamma\gamma$ mass spectra after the last ("Veto") cut for several m_P intervals. It is clearly seen that the π° signal survives only for the region of the $\pi^-\pi^\circ(\pi^\circ)$ decay. This situation allows to perform an effective background subtraction procedure:

the $m(\gamma\gamma)$ spectra for different intervals of the missing mass with 10 MeV bin size, starting from zero, have been fitted by the sum of the Gaussian (with the fixed width of 9.3 MeV and the fixed mass of 135 MeV) and quadratic (or linear) polynomial. Such fits are also shown in Fig. 6(right half). The obtained numbers of π^0 as a function of m_P form the "filtered" missing mass spectrum shown in Fig.7.

3 Analysis and results

In order to calculate the upper limits the "filtered" missing mass distribution has been fitted by the sum of the signal Gaussian with a fixed width of $\sigma = 11.1$ MeV, as determined from the signal MC and a background. The background has been described by two components: the Gaussian for the $\pi^-\pi^0(\pi^0)$ peak and a constant background. Fig.7 shows an example of such a fit for the signal at $m_P = 5$ MeV. The events upper limits at the 90% confidence level are calculated as

$$N_{UL} = max(N_{sig}, 0) + 1.28 \cdot \sigma \quad , \tag{3}$$

where N_{sig} is the number of events in the signal Gaussian and σ is the error estimate for N_{sig}. The signal upper limit UL is calculated as

$$UL = \frac{N_{UL} \cdot 0.2116 \cdot \varepsilon(K_{\pi 2})}{N(K_{\pi 2}) \cdot \varepsilon} \qquad (4)$$

with 0.2116 equal to the branching ratio $Br(K_{\pi 2})$, and $N(K_{\pi 2})$ equal to the number of reconstructed $K^- \to \pi^- \pi^\circ$ decays found to be ~ 1.5 M events for the first run and ~ 4.5 M events for the second run. The values ε and $\varepsilon(K_{\pi 2})$ are respective efficiencies for $K^- \to \pi^- \pi^\circ\ P$ and $K_{\pi 2}$ decays, which include both the reconstruction efficiency and geometrical acceptance. The signal efficiency ε rises monotonically from $\sim 3.3\%$ to $\sim 11.3\%$ in the mass interval from 0 to 170 MeV and then drops slightly to the value $\sim 10.3\%$ at 200 MeV. The values for two runs are practically the same. The $K_{\pi 2}$ efficiency $\varepsilon(K_{\pi 2})$ is equal to 17.49 % for the first run and 24.92 % for the second run.

The weighted average ratio $\varepsilon/\varepsilon(K_{\pi 2})$ with the weights proportional to the runs statistics has been used for the combined data sample.

The final results obtained using combined statistics of two runs are given in Fig. 8. Left part of this figure shows a comparison of our result with that published by the E787 collaboration [2].

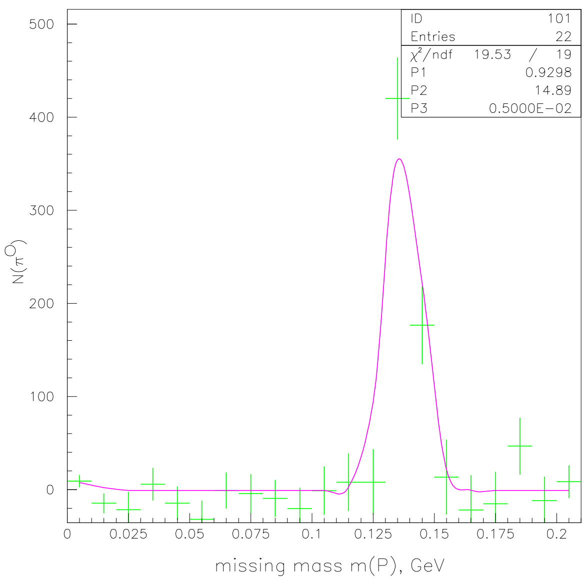

Figure 7: The number of π° from the fit of the corresponding m($\gamma\gamma$) mass spectrum versus the missing mass M_P, run1+run2 data. The curve is the result of the fit with a signal at $m_P = 5$ MeV plus background.

Systematic uncertainty in the obtained upper limits have been determined by variation of the selection criteria, changing the bin size of the missing mass intervals, etc. It is found to be ~ 25 — 30 %.

The obtained upper limits can be transformed into the limits on the value of the modulus $|h_{12}^D|$ (see equation 2). The corresponding limits are compared in Fig. 8 (right part) with the theoretical limit evaluated using $K_L - K_S$ mass difference.

4 Summary and conclusions

A search for a possible pseudoscalar sgoldstino production in the decay $K^- \to \pi^- \pi^\circ P$ has been performed. It was assumed that sgoldstino decays outside the setup, i.e. is invisible. No signal is seen in the m_P mass interval between 0 and 200 MeV. The obtained 90% confidence upper limits are $\sim 8.0 \cdot\ 10^{-6}$ for the sgoldstino mass range of $0 \div 200$ MeV, excluding the interval near $m(\pi^\circ)$, where the limit is $\sim 3.0 \cdot\ 10^{-5}$. These results improve the confidence limits published by the E787

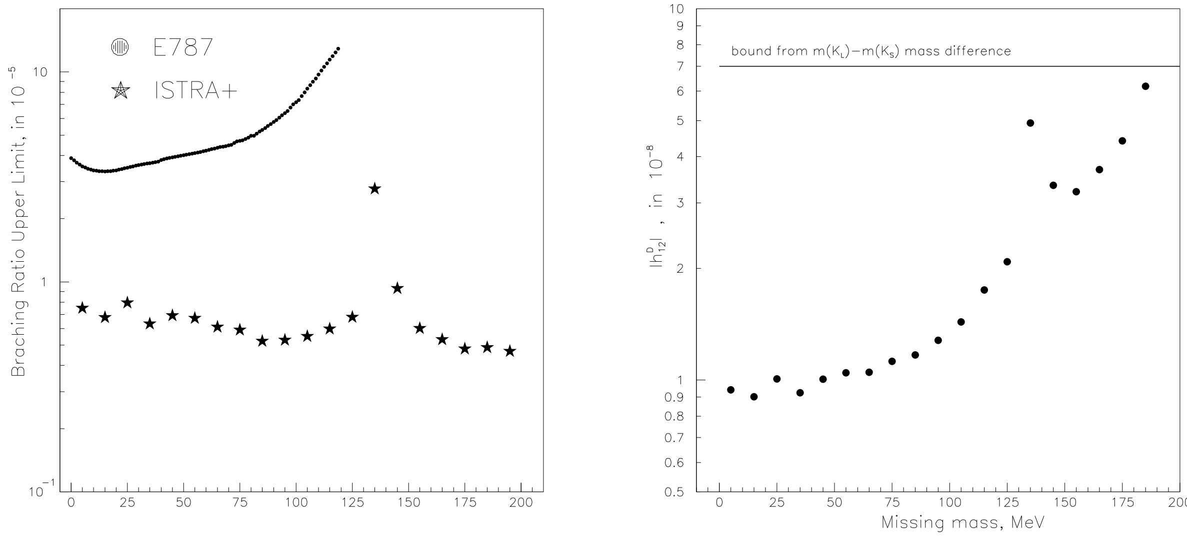

Figure 8: Mass dependence of the upper limits (left figure), calculated using two runs together and the bounds on the $|h_{12}^D|$ (right figure) compared with the theoretical limit from $K_L - K_S$ mass difference.

Collaboration. Our limits improve also the theoretical constraints on $|h_{12}^D|$ evaluated using $K_L - K_S$ mass difference.

In future, we plan to extend our search for a sgoldstino signal in the scenario when the decay $P \to \gamma\gamma$ happens inside the setup.

The authors would like to thank D.S. Gorbunov, V.A. Matveev and V.A. Rubakov, for numerous discussions. We specially thank D.S. Gorbunov for the help with calculations of the matrix element for sgoldstino production.

The work is supported by the RFBR grant N03-02-16330.

References

[1] D.S. Gorbunov and V.A. Rubakov, Phys. Rev. **D64** (2001) 054008.

[2] S. Adler et al., E787 Collaboration, Phys. Rev. **D63** (2001) 032004.

[3] L. Littenberg, Rare kaon and pion decays, Lectures given at the PSI Summer School on Particle Physics, Zuoz, 2002, PSI Proceedings 03-02, March 2003, preprint hep-ex/0212005.

[4] I.V. Ajinenko et al., First results on a search for light pseudoscalar sgoldstino in K^- decays, preprint hep-ex/0212060, 2002.

[5] I.V. Ajinenko et al., Phys.Atom.Nucl. 65(2002) 2064; Yad. Fiz. 65(2002)2125.

[6] I.V. Ajinenko et al., Phys.Atom.Nucl. 66(2003) 105; Yad. Fiz. 66(2003) 107.

[7] I.V. Ajinenko et al., Phys. Lett. **B567** (2003) 159.

[8] R. Brun et al, CERN-DD/EE/84-1, CERN, Geneva, 1984.